Impact of Torsion Angles to Tune Efficient Dye-Sensitized Solar Cell/Donor–π–Acceptor Model Containing Triphenylamine: DFT/TD-DFT Study

F. Bahrani, R. Hameed,
S. Resan and M. Al-anber*

Molecular Engineering and Computational Modeling Lab, Department of Physics, College of Science, University of Basrah, Karmat-Ali Road, 261004, Basrah, Iraq

Received: 25.11.2021 & Accepted: 15.03.2022

Doi: 10.12693/APhysPolA.141.561 *e-mail: mohanned.mohammed@uobasrah.edu.iq

The molecular design of a donor–linker–acceptor based on triphenylamine as a donor group linked with the acceptor cyanoacrylic acid via 2,2'-bithiophene as π-conjugation has been studied for a dye-sensitized solar cell. In this work, the dihedral angle between the donor or the acceptor group and the π-spacer has been rotated. The performance of the molecular design has been investigated computationally, using density functional theory at the B3LYP/6-311G(d,p) theory level, and the effect of tuning torsion angles on the parameters of the solar cells has been studied. To evaluate the effect of tuning torsion angles on photovoltaic properties, the HOMO and LUMO energy levels, optical bandgap energy, oscillator strength, light-harvesting efficiency, excited state lifetime, injection driving force, regeneration driving force, open-circuit voltage, and fill factor have been determined. The results reveal that the molecular design properties that result from the rotation of the dihedral angles can show excellent performance for DSSCs compared to the original dye molecule.

topics: dye-sensitized solar cells, donor–π–acceptor, absorption spectrum, torsion angles

1. Introduction

Renewable energy technology has been developed and optimized by many researchers to produce sustainable, reliable, and clean energy. Solar cells are considered to be an alternative renewable energy source. Dye-sensitized solar cells (DSSCs) as organic solar cells are one of the most effective photovoltaic devices due to easy fabrication, low cost, raw materials abundance, molecular design flexibility, being a higher molecular extinction coefficient device, long life, and large-area preparation [1, 2]. DSSCs have enormous potential for commercial applications [2]. The first report on DSSCs, by O'Regan and Grätzel, was published in 1991 [1]. To date, the reported research on DSSCs reveals that the conversation efficiency has reached up to 14.4% [3, 4].

The configuration of metal-free organic dyes for a donor–π–acceptor (D-π-A) is a push-pull structure in the form of a dipolar, electron-donor, π-bridge spacer, and electron-acceptor. In particular, a DSSC is composed of a semiconductor with a wide bandgap, commonly TiO_2 as an anode, molecular dye, a redox electrolyte, commonly I^-/I_3^- as an electron mediator (between the TiO_2 and the electrode), and a counter-electrode, usually platinum (Pt), as a cathode. In general, a typical DSSC operation [5–7] is that the incident light absorbed by the dye sensitizer anchored on the TiO_2 semiconductor surface gets excited; after that, the excited electrons are injected into the conduction band edge (E_{CB}) of the semiconductor, and the dye molecule becomes oxidized. Subsequently, the charge separation occurs at the interface of the dye and the semiconductor through the photo-induced electron injection process [1, 8]. The oxidized dye is regenerated by regaining electrons from the I^- ion redox mediator, which gets oxidized to I_3^-. The oxidized I_3^- is reduced to I^- by getting electrons from the electrode [6].

In the D-π-A structure, understanding the charge-transporting properties of the molecular structure of a DSSC is based on the relationship between donor, acceptor, and spacer parts. The donor part has a significant role in tuning, modifying the absorption spectra, and controlling the molecular energy levels and intramolecular charge separation [9]. Coumarin [10], indoline [11], carbazole [12, 13], and triphenylamine derivatives (TPA) [14, 15] have been utilized as a donor part in DSSCs. TPA could enhance the light absorption ability of the molecular dye, and it has a non-planar structure that inhibits the dye aggregation on

the TiO_2 semiconductor surface [16, 17]. Moreover, TPA displays excellent solubility, great stability, and high photo-luminescent efficiency [18]. In addition, it is used extensively in the optoelectronic fabrication of electronic devices, such as DSSCs [19], organic light-emitting diodes (OLEDs) [20], and field-effect transistors (OFETs) [21]. Furthermore, TPA represents an ideal donor part in DSSC since it has excellent electron-donating and high hole-transporting capability [22]. However, cyanoacrylic acid (CA) is commonly employed as an anchoring group for DSSCs. Due to the strong electron-withdrawing characteristics of cyanide groups, they are specifically utilized in D-π-A organic dye [23], and they also play the dual role of acceptor and anchor [24]. The strong binding of CA on the semiconductor surface (TiO_2) facilitates the process of electron injection [25]. In contrast, enhancing the absorption of the light in DSSC can be attributed to the spacer part since it helps to transfer the charge faster from the ground to the excited state and absorbs the light at a longer wavelength. It has been proved that the thiophene moiety is a better π-conjugated spacer because of increases in the intramolecular charge transfer (ICT) efficiency and promotes the intensity of absorption [26]. No studies show the role of the tuning torsion angles for D-π-A as a solar cell molecular design between the donor or the acceptor part and the π-spacer. Therefore, in this work, the impact of rotating the dihedral angle between the donor or the acceptor part and the π-spacer has been illustrated. The D-π-A molecular design has been investigated theoretically to understand the effect of tuning torsion angles on the photovoltaic parameters, using density functional theory (DFT) at the B3LYP/6-311G(d,p) and the differences in the DSSC efficiency.

2. Computational methods

The molecular design of a DSSC consists of TPA and CA as the donor and acceptor groups, respectively, linked by 2,2'-bithiophene as a π-conjugation bridge (π-spacer), as shown in Fig. 1. For the D-π-A block, the dihedral angle between the donor (D) and the π-bridge is $\theta_{\text{D-}\pi}$, whereas $\theta_{\text{A-}\pi}$ represents the dihedral angle between the acceptor (A) and the π-bridge. In this paper, the dihedral angles of the dye molecule D-π-A structure have been rotated either by rotation of the donor part around the stationary spacer–acceptor part ($\theta_{\text{D-}\pi}$) or by the rotation of the acceptor part around the stationary spacer–donor part ($\theta_{\text{A-}\pi}$). The molecular design has been investigated to explore the influence of the torsional angles on the properties of the DSSC. The rotation of the dihedral angles in the right (positive) and left (negative) direction have been studied. The dihedral angles $\theta_{\text{A-}\pi}$ and $\theta_{\text{D-}\pi}$ have been rotated within the range of 0–90° by an increment of 10° for both directions. In general, all the possible torsional angles have been studied to find the influence of each rotated angle on the photovoltaic properties. The ground state geometry optimizations for the D-π-A block have been performed with the Gaussian09 program package, using the density functional theory (DFT) [27, 28] at the hybrid function of the exchange correlation B3LYP (Becke three-parameter Lee–Yang–Parr) theory level [28] with 6-311G(d,p) basis sets for C, H, O, N, and S. The torsion angles and the optoelectronic properties of the D-π-A compounds have been calculated using the time-dependent density functional theory (TD-DFT) method [29] with B3LYP/6-311G(d,p) basis sets for all atoms, based on the optimized ground state geometry. The oscillator strengths and excited state energies have been evaluated using TD-DFT calculations.

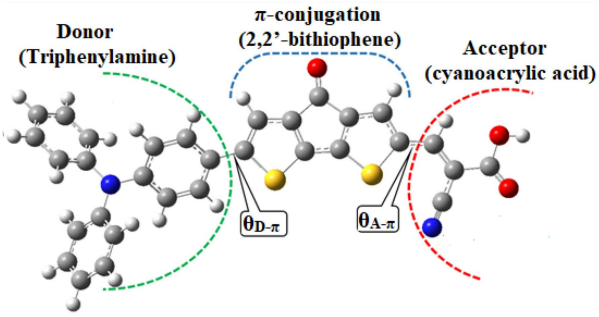

Fig. 1. General molecular design DSSC consisting of donor and acceptor groups with a π-conjugation bridge in the present work.

As for the geometry of the D-π-A structure, it was optimized by DFT using B3LYP with a 6-311G(d,p) basis, where the dihedral angle values ($\sim 25°$ and $\sim 0°$) for the TPA and CA with the thiophene rings of a π-bridge moiety, respectively, were in agreement with the previous report of Fahim et al. [18]. In all calculations, the gas phase was assumed. During the scanning process, the geometrical parameters were simultaneously relaxed, so they changed for both directions between 0 and 90° in 10° steps.

3. Results and discussion

3.1. Ground state geometry

The variation of relative stability ΔE_t for molecule studies (D-π-A) with the dihedral angles $\theta_{\text{A-}\pi}$ and $\theta_{\text{D-}\pi}$ are shown in Fig. 2. The rotation of $\theta_{\text{D-}\pi}$ shows little difference in energies compared with $\theta_{\text{A-}\pi}$, which may need high levels of energy. Therefore, $\theta_{\text{D-}\pi}$ has a high probability of occurring in D-π-A. In addition, the energy for the left direction of $\theta_{\text{D-}\pi}$ is relativity lower than that for the right direction of each specific dihedral angle. Generally, the implied $\theta_{\text{D-}\pi}$ has a more stable structure than $\theta_{\text{A-}\pi}$. However, it should be noted that the barriers of torsional angles are not very high compared to the results of Resan et al. [30].

3.2. Frontier molecular orbitals and energy levels

In this work, the D-π-A organic molecular dye has been rotated with the different torsional angles $\theta_{\text{A-}\pi}$ and $\theta_{\text{D-}\pi}$. For the donor and acceptor groups, the HOMO and the LUMO energy band levels are substantial factors that need to be examined to see whether effective charge transfer will occur between the donor and the acceptor. The HOMO and LUMO energy levels have been determined using the B3LYP/6-311G(d,p) to evaluate the electronic and transition properties of the dyes. Designing an efficient dye for DSSCs requires that this dye has LUMO energy levels localized higher than the TiO_2 semiconductor E_{CB} (-4.0 eV) [31], and HOMO energy levels should be localized lower than the redox potential of the electrolyte I^-/I_3^- (-4.80 eV). The maximum value of the E_{HOMO} molecule energy levels is more sensitive to electron donation, while the minimum value of the lower unoccupied molecular orbital energy levels (E_{LUMO}) is responsible for electron reception.

The calculated HOMO and LUMO levels of $\theta_{\text{A-}\pi}$ and $\theta_{\text{D-}\pi}$ are shown in Fig. 3. The acceptor rotation $\theta_{\text{A-}\pi}$ leads to an increase in the upper occupied molecular orbital energy (E_{HOMO}), indicating that this rotation requires high levels of energy (see Fig. 2). However, the donor rotation $\theta_{\text{D-}\pi}$ generally reduces E_{HOMO} slightly. Since the donor rotation has a high probability of occurring, especially on the left (see Fig. 2), this will increase E_{HOMO}. The dihedral angles show that HOMO energy level orbitals are localized below the electrolyte I^-/I_3^- (-4.80 eV), as shown in Fig. 3, which means that the oxidized dyes are able to restore the electrons from the redox potential. Figure 3 shows that only E_{LUMO} varies with the acceptor rotation $\theta_{\text{A-}\pi}$ and pulls up the LUMO. The results show that LUMO energy level orbitals are above the E_{CB} of TiO_2 (-4.0 eV), indicating that the designed molecular dye, when rotating the dihedral angles, can efficiently inject electrons into the TiO_2 conduction band edge. The highest LUMO values are for $\theta_{\text{A-}\pi}$, which enhances the open-circuit voltage (V_{OC}) and the injection driving force (ΔG_{inj}), while the lowest HOMO values are for $\theta_{\text{D-}\pi}$ in the left direction, particularly when enhancing the regeneration driving force (ΔG_{reg}). Importantly, before the rotations, the values of HOMO (-5.45 eV) and LUMO (-3.32 eV) were in agreement with the previous report of Fahim et al. [18].

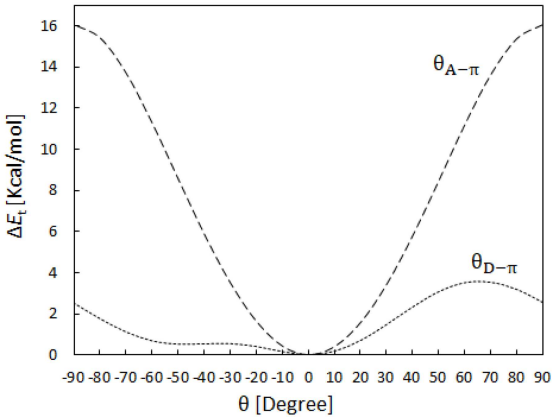

Fig. 2. The angular variation of relative stability ΔE_t for dye molecule (D-π-A) with dihedral angles ($\theta_{\text{A-}\pi}$ and $\theta_{\text{D-}\pi}$).

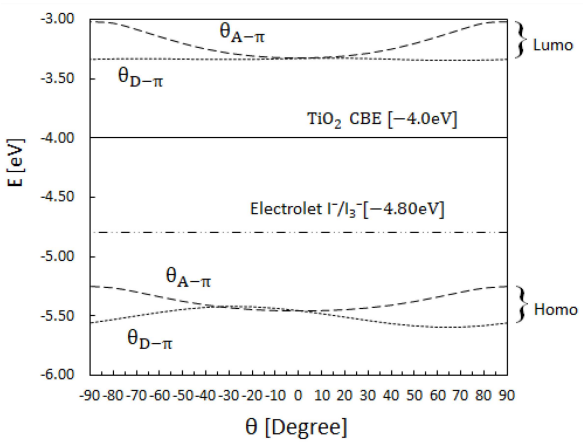

Fig. 3. The angular variation of E_{HOMO} and E_{LUMO} for the dye molecule (D-π-A) with dihedral angles ($\theta_{\text{A-}\pi}$ and $\theta_{\text{D-}\pi}$).

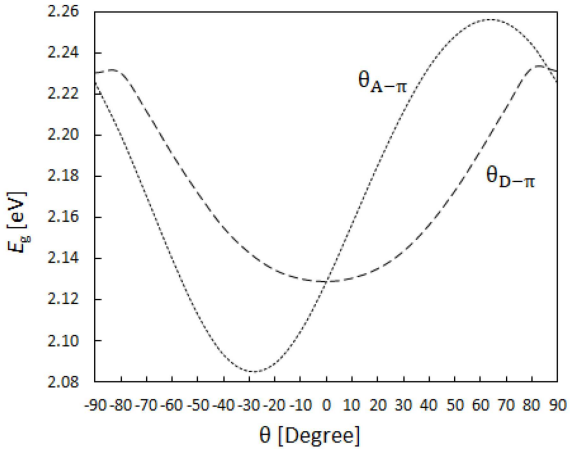

Fig. 4. The angular variation of the energy gap for dye molecule (D-π-A) with dihedral angles ($\theta_{\text{A-}\pi}$ and $\theta_{\text{D-}\pi}$).

The qualifying quality in DSSC for the energy bandgap E_g suggests that the $E_{\text{LUMO}} - E_{\text{HOMO}}$ energy should be small to allow a redshift wavelength to be absorbed and enhance the light-harvesting efficiency (LHE) [23, 32]. The minimum bandgap for torsional angles (Fig. 4) is $\theta_{\text{D-}\pi}$ on the left side, mostly in the range of 0–30°; this can occur due to the relative stability in Fig. 2. The lower energy bandgap value of the system has a significant effect on the ICT, which leads to a redshift absorption spectrum. Therefore, $\theta_{\text{D-}\pi}$ on the left

side has the lowest bandgap compared with others, which indicates that the absorption spectrum possibly has shifted to red, thus promoting sunlight harvesting in the long-wavelength region. It has been reported [18] that the bandgap before the rotations of the D-π-A structure consists of TPA-donor, CA-acceptor, and 2,2'-bithiophene as π-spacer, and its value was 2.26 eV, calculated using the conductor-like polarizable continuum model (CPCM) at the B3LYP/6-311G(d,p) level of theory. This result agrees with our results (2.13 eV), and the difference in results can be attributed to the difference in the computational model used.

3.3. Photovoltaic properties

The key parameters to characterise the photovoltaic performance of DSSCs are V_{OC}, LHE, ΔG_{inj}, ΔG_{reg}, fill factor (FF), and the excited state lifetime (τ). DFT has been utilized to identify the impact of these parameters on an efficient device when rotating the dihedral angles ($\theta_{A\text{-}\pi}$ and $\theta_{D\text{-}\pi}$).

3.3.1. Light-harvesting efficiency

The DSSC performance is related to the dye responsible for the incident light [33]. The LHE is the light absorbed by the dye-sensitized semiconductor film (commonly TiO_2). The Beer–Lambert law proposes that the LHE of a cell relies on the coefficient of dye extinction, the concentration of dye, and the optical path length within the semiconductor film [34]. The LHE, another important factor that affects the short circuit current J_{SC}, is expressed as [35]

$$\mathrm{LHE}(\lambda) = 1 - 10^{-f}, \tag{1}$$

where LHE(λ) is the light-harvesting efficiency at a given wavelength and f is the oscillator strength of the adsorbed dye molecule related to λ_{max}. In order to maximize the photocurrent response by increasing the ability of light to capture and then promote cell performance [36], the LHE values of the dyes have to be as high as possible [33]. Therefore, a small energy gap and a relatively high LHE are useful for achieving a redshift [23, 32]. Increasing the LHE will enhance the J_{SC} value, and this will result in solar cell efficiency [37]. The LHE is directly associated with the oscillator strength of the adsorbed dye molecule [1].

The theoretical values of the LHE for $\theta_{A\text{-}\pi}$ and $\theta_{D\text{-}\pi}$ are shown in Fig. 5. In general, the LHE values of $\theta_{A\text{-}\pi}$ are greater than those of $\theta_{D\text{-}\pi}$ for each specific angle on the right, while the values of LHE for $\theta_{D\text{-}\pi}$ are higher than those of $\theta_{A\text{-}\pi}$ for each specific angle on the left. The LHE values of $\theta_{D\text{-}\pi}$ on the left are higher than those of $\theta_{A\text{-}\pi}$ on the right for each specific angle due to the fact that the energy bandgap is smaller for $\theta_{D\text{-}\pi}$ on the left than that of $\theta_{A\text{-}\pi}$ on the right. The highest value for f and LHE implies that the donor rotation could absorb more photons thanks to the J_{SC} being maximized. It has been found using B3LYP/6-31G(d) [38] that LHE

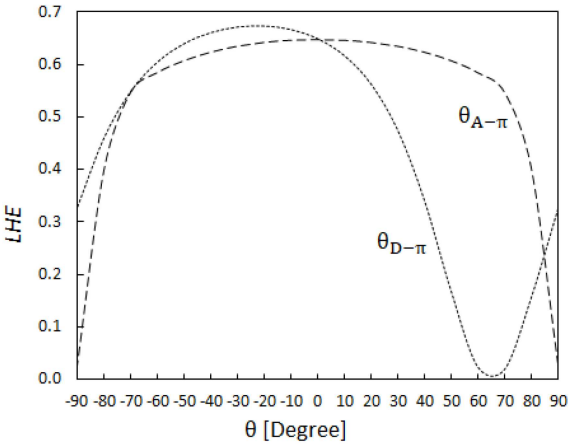

Fig. 5. The angular variation of LHE for the dye molecule (D-π-A) with dihedral angles ($\theta_{A\text{-}\pi}$ and $\theta_{D\text{-}\pi}$).

before the rotations of the D-π-A structure consists of TPA-donor, CA-acceptor, and 2,2'-bithiophene as π-spacer, and its value was 0.976. This result agrees with our result (0.65), and the difference in values can be attributed to the difference in the basis set.

3.3.2. Excited state lifetime

The fundamental parameter needed to examine the charge transfer efficiency is the lifetime of the first excited state [39], where the performance of the electron injection from the excited dye into the TiO_2 E_{CB} semiconductor is determined by the lifetime of the excited state [9]. In a short lifetime, the electrons injected into the TiO_2 E_{CB} semiconductor are ultrafast, thus allowing electron recombination [9]. This process will reduce the photovoltaic performance because of a decrease in the efficiency of the charge collection through the minimization of the J_{SC} and photoelectric conversion efficiency (PCE) [9]. A longer lifetime of the dye means that it remains stable for a longer time in the cationic state (excited state), which facilitates the transfer of the charge, thus enhancing the J_{SC} [39]. The excited state lifetime τ of the dye can be determined as [35]

$$\tau = \frac{1.499}{f}\frac{1}{(E^*)^2}, \tag{2}$$

where E^* is the excitation energy [cm^{-1}] of the different electronic states.

The lifetime values as a function of the rotation angles ($\theta_{A\text{-}\pi}$ and $\theta_{D\text{-}\pi}$) are shown in Fig. 6. Figure 6 shows that for $\theta_{A\text{-}\pi}$, there is no perceptible change in τ values for each specific angle between the right and left directions, which is also due to the relative stability in Fig. 2. The lifetime value of $\theta_{D\text{-}\pi}$ is higher beyond the right rotation angle, which is approximately equal to 40° and its peak is at 70°, while the left rotation does not show any near

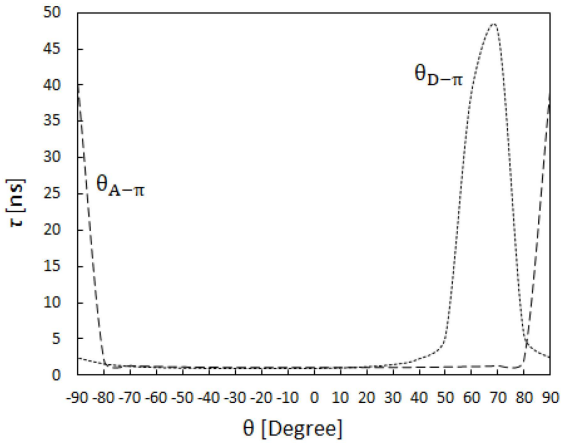

Fig. 6. The angular variation of lifetime for the dye molecule (D-π-A) with dihedral angles ($\theta_{\text{A-}\pi}$ and $\theta_{\text{D-}\pi}$).

influences. This implies that $\theta_{\text{D-}\pi}$ in the right direction would remain stable in the excited state for a long time, generating a higher efficiency of charge transfer by delaying the process of charge recombination. This is suitable for improving the efficiency of the DSSC [39].

3.3.3. Driving force for electron injection and dye regeneration

In DSSC, the injection driving force (ΔG_{inj}) is a significant factor affecting the injection of the electron [9]. The rate of electron injection from the dye into the TiO_2 E_{CB} is useful in examining photovoltaic performance. Here, ΔG_{inj} represents the injection driving force of the electron injected from the dye excited state LUMO level into the conduction band of the semiconductor oxide [27]. The negative sign of ΔG_{inj} suggests the spontaneity of the process [1]. According to Preat's method [40], ΔG_{inj} can be determined as follows [36]

$$\Delta G_{\text{inj}} = E^*_{\text{dye}} - E_{\text{CB}}(\text{TiO}_2), \tag{3}$$

where E^*_{dye} is the oxidation potential energy of the dye molecule in the excited state. It can be determined as [41]

$$E^*_{\text{dye}} = E_{\text{dye}} - E_{0-0}, \tag{4}$$

where E_{dye} is the oxidation potential of the dye molecule in the ground state and E_{0-0} is the electronic vertical transition energy associated with λ_{max}. In general, more negative values (the higher absolute value) of ΔG_{inj} lead to a better charge transfer possibility and a faster electron injection, and this enhances the J_{SC} [9]. It has been reported that to effectively convert solar energy to current, $E_{\text{dye}*}$ (LUMO) should be at least 0.5 eV higher than E_{CB}, while E_{dye}(HOMO) should be at least 0.2 eV lower than the redox electrolyte [42, 43].

The theoretically calculated results of ΔG_{inj} for $\theta_{\text{A-}\pi}$ and $\theta_{\text{D-}\pi}$ are shown in Fig. 7a.

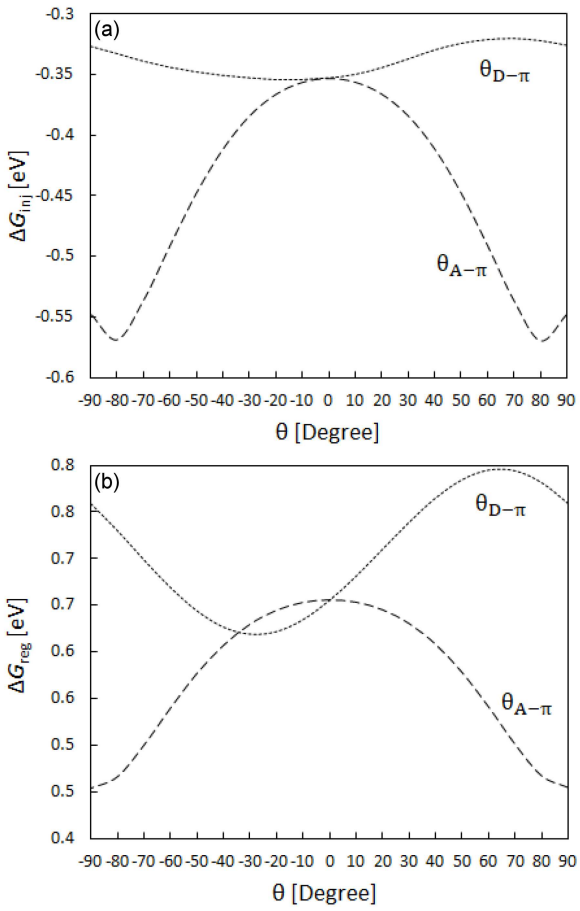

Fig. 7. The angular variation for the dye molecule (D-π-A) with dihedral angles ($\theta_{\text{A-}\pi}$ and $\theta_{\text{D-}\pi}$) for (a) the injection driving force (ΔG_{inj}) and (b) the regeneration driving force (ΔG_{reg}).

All the calculated ΔG_{inj} values for torsional angles have negative sign values, which means that the electron injection from the dye in an excited state into the E_{CB} of the semiconducting oxide (TiO_2) is spontaneous in nature [1]. All ΔG_{inj} values have less negative potential than that of the TiO_2 E_{CB} (−4.0 eV), which implies that the excited state of sensitizer dye lies above the E_{CB} of the TiO_2 semiconductor, thus enhancing the injection of electrons from the excited dyes into the semiconductor. The acceptor rotation, $\theta_{\text{A-}\pi}$, shows a big increase in the ΔG_{inj} values for right and left rotations, but, as shown in Fig. 2, these rotations need high levels of energy. Generally, the rotation of the acceptor group can enhance the rate of the electron injection from the dye into the TiO_2 E_{CB} (higher J_{SC}) semiconductor and embellish the photovoltaic performance. Meanwhile, the donor group rotation $\theta_{\text{D-}\pi}$ did not show any interesting effects on the ΔG_{inj} values. It has been reported [38] that the value of ΔG_{inj} before the rotations of TPA-donor, CA-acceptor, and 2,2'-bithiophene as π-spacer, was −0.8 eV, calculated using B3LYP/6-31G(d). This result, in fact, agrees with our result.

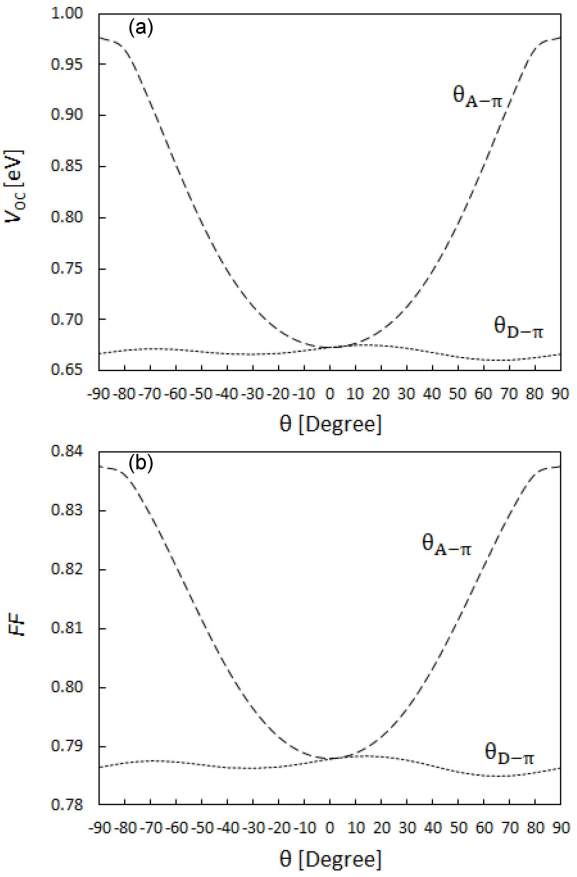

Fig. 8. The angular variation for the dye molecule (D-π-A) with dihedral angles ($\theta_{A\text{-}\pi}$ and $\theta_{D\text{-}\pi}$) of (a) open-circuit voltage (V_{OC}) (b) fall factor (FF).

The fundamental process in DSSCs is dye regeneration, in which absorbed solar energy is converted to current [1]. It should be noted that ΔG_{reg} is an essential operator impacting the photoelectric conversion efficiency (PCE) [44]. The driving force of dye regeneration ΔG_{reg} is another important factor that affects the J_{SC} [9]. The large driving forces of dye regeneration enhance the regeneration efficiency, which promotes the increase of J_{SC} [44]. Furthermore, ΔG_{reg} is defined as the difference in the potential energy between the HOMO of the dye molecules and the redox potential of the applied electrolyte, which can be calculated as follows [45]

$$\Delta G_{reg} = E_{redox} - E_{dye}. \quad (5)$$

Here, E_{redox} is the redox potential of the electrolyte. Iodide/triiodide (I^-/I_3^-) is typically used as the electrolyte; the level of the coupled redox electrolyte (I^-/I_3^-) is about −4.80 eV [27]. A lower ΔG_{reg} leads to a higher recombination efficiency [1]. The increase in the HOMO results in a decrease in ΔG_{reg}. Figure 7b shows the calculated results for ΔG_{reg} as a function of the torsional angles, where the increase in the acceptor group rotation, $\theta_{A\text{-}\pi}$, reduces the ΔG_{reg}. Meanwhile, for $\theta_{D\text{-}\pi}$ the values on the left are mostly lower than those on the right for each specific angle — this is because the HOMO levels on the right are generally lower than those of the left direction for each specific angle (see Fig. 3). Note that $\theta_{D\text{-}\pi}$ has a larger ΔG_{reg} in the right direction for each specific angle, which can improve dye regeneration and cause a higher photocurrent generation. In addition, V_{OC} will be higher because of the reduction in the recombination between the injected electrons and the photo-oxidized dye molecules.

3.4. Open-circuit voltage and fill factor

One of the key factors in a DSSC is V_{OC}, which can be approximately determined as [1]

$$V_{OC} = E_{LUMO} - E_{CB}(TiO_2). \quad (6)$$

To obtain a higher V_{OC} value, the E_{LUMO} must be as high as possible [9]. Should the photo-generated electrons be transferred more quickly to TiO_2 E_{CB}, the recombination of electrons and the oxidized ionic species of the electrolyte would result in upward photo-voltage.

A higher V_{OC} enhances photovoltaic performance. The V_{OC} values in DSSC can be estimated approximately by the energy difference between E_{LUMO} of the dye and E_{CB} of TiO_2, considering the energy lost through the photo charge generation [26].

The calculated values of V_{OC} are shown in Fig. 8a. For any donor group rotation angle, $\theta_{D\text{-}\pi}$, there is no noticeable change in the V_{OC} values in the right and left direction, since the values of E_{LUMO} are nearly the same in both directions for each specific angle. As there is a chance to increase the $\theta_{A\text{-}\pi}$, the value of V_{OC} can increase too. The calculated values of V_{OC} suggest that the molecular dyes could be utilized as sensitizers, since the process of electron injection from the excited molecule into the E_{CB} of TiO_2 is possible.

The FF played a leading role in device efficiency, and the ideal value of the FF is equal to 1 [46]. The FF can be determined as [46]

$$FF = \frac{V_{OC} - \ln\left(V_{OC} + 0.72\right)}{V_{OC} + 1}. \quad (7)$$

For $\theta_{A\text{-}\pi}$, the FF values are approximately the same in the right and left directions for each specific angle. The values of the FF increased as the $\theta_{A\text{-}\pi}$ increased. Generally, the FF with torsional angles had highest value for $\theta_{A\text{-}\pi}$ compared to $\theta_{D\text{-}\pi}$ (Fig. 8b).

4. Conclusion

The designed DSSC, based on donor TPA linked with the acceptor CA by 2,2'-bithiophene as π-conjugation, has been theoretically elucidated using DFT. The molecular design resulting from the rotation of the dihedral angle has been investigated computationally at the B3LYP/6-311G(d,p) theory level. The molecular design for the dihedral angles $\theta_{D\text{-}\pi}$ can occur easily in the left direction, and it has a significant effect on ICT by having lower optical bandgap energy. All the torsional angles of $\theta_{A\text{-}\pi}$

or $\theta_{\text{D-}\pi}$ have HOMO and LUMO energy levels that guarantee the energetically favourable dye regeneration and electron injections. In addition, the electron injection from the dye into the TiO_2 is spontaneous for all the torsional angles because of a negative value of ΔG_{inj}. The donor group rotations have the highest ΔG_{reg}, LHE, τ, and lower optical bandgap energy. This leads to the facilitation of the charge transfer by a reduction of the charge recombination and enhancement of the dye regeneration, which in turn leads to a higher photocurrent generation by the conversion of more light to electrical power, and then improvement of solar cell efficiency. It can be concluded that the influence of the tuning torsion angles positively affects the efficiency of the photovoltaic properties and thus improves the device's performance.

References

[1] A. Saha, B. Ganguly, *RSC Adv.* **10**, 15307 (2020).

[2] F. Xu, T.T. Testoff, L. Wang, X. Zhou, *Molecules* **25**, 4478 (2020).

[3] L. Zhang, X. Yang, W. Wang et al., *ACS Energy Lett.* **4**, 943 (2019).

[4] Y.K. Eom, S.H. Kang, I.T. Choi, Y. Yoo, J. Kim, H.K. Kim, *J. Mater. Chem. A* **5**, 2297 (2017).

[5] L.A. Kosyachenko, *Solar Cells: Dye-Sensitized Devices*, IntechOpen, London 2011.

[6] T. Le Bahers, T. Pauporté, P.P. Lainé, F. Labat, C. Adamo, I. Ciofini, *J. Phys. Chem* **4**, 1044 (2013).

[7] Y. Jiao, F. Zhang, S. Meng, in: *Solar Cells: Dye-Sensitized Devices*, Ed. L. Kosyachenko IntechOpen, London 2011.

[8] A. Mishra, M.K.R. Fischer, P. Bäuerle, *Angew. Chemie Int. Ed.* **48**, 2474 (2009).

[9] M.A.M. Rashid, D. Hayati, K. Kwak, J. Hong, *Nanomaterials* **10**, 914 (2020).

[10] R. Sánchez-De-Armas, M. Á. San Miguel, J. Oviedo, J.F. Sanz, *Phys. Chem. Chem. Phys.* **14**, 225 (2012).

[11] B. Liu, Q. Liu, D. You, X. Li, Y. Naruta, W. Zhu, *J. Mater. Chem.* **22**, 13348 (2012).

[12] K. Srinivas, C.R. Kumar, M.A. Reddy, K. Bhanuprakash, V.J. Rao, L. Giribabu, *Synth. Met.* **161**, 96 (2011).

[13] A. Venkateswararao, K.R.J. Thomas, C.P. Lee, C.T. Li, K.C. Ho, *ACS Appl. Mater. Interfaces* **6**, 2528 (2014).

[14] S. Kotteswaran, P. Ramasamy, *New J. Chem.* **45**, 2453 (2021).

[15] P. Pounraj, V. Mohankumar, M.S. Pandian, P. Ramasamy, *AIP Conf. Proc.* **2115**, 030345 (2019).

[16] Z. Yang, D. Wang, X. Bai, C. Shao, D. Cao, *RSC Adv.* **4**, 48750 (2014).

[17] M. Yahya, A. Bouziani, C. Ocak, Z. Seferoğlu, M. Sillanpää, *Dyes Pigm.* **192**, 109227 (2021).

[18] Z.M.E. Fahim, S.M. Bouzzinea, M.M. Hamidic, M. Bouachrined, M. Hamidia, G. Salgado-Moráne, L.H. Mendoza-Huizarf, G.A. Alvarez-Romerof, *Quim. Nova* **41**, 129 (2018).

[19] P. Agarwala, D. Kabra, *J. Mater. Chem. A* **5**, 1348 (2017).

[20] J. Zhang, Y. Yang, C. He, Y. Li, *Sci. China Chem.* **54**, 695 (2011).

[21] C. Bathula, A.B. Appiagyei, H. Yadav et al., *Nanomaterials* **9**, 1787 (2019).

[22] M. Adnan, J. Iqbal, S. BiBi, R. Hussain, M.N. Akhtar, M.A. Rashid, B. Eliasson, K. Ayub, *Z. Phys. Chem.* **231**, 1127 (2017).

[23] S. El Mzioui, S.M. Bouzzine, İ. Sidir, M. Bouachrine, M.N. Bennani, M. Bourass, M. Hamidi, *J. Mol. Model.* **25**, 1 (2019).

[24] P. Cowper, A. Pockett, G. Kociok-Köhn, P.J. Cameron, S.E. Lewis, *Tetrahedron* **74**, 2775 (2018).

[25] K. Srinivas, K. Yesudas, K. Bhanuprakash, V.J. Rao, L. Giribabu, *J. Phys. Chem. C* **113**, 20117 (2009).

[26] M. Hachi, S. El Khattabi, A. Fitri, A.T. Benjelloun, M. Benzakour, M. Mcharfi, M. Hamidi, M. Bouachrine, *J. Mater. Environ. Sci.* **9**, 1200 (2018).

[27] P.N. Samanta, D. Majumdar, S. Roszak, J. Leszczynski, *J. Phys. Chem. C* **124**, 2817 (2020).

[28] B. Miehlich, A. Savin, H. Stoll, H. Preuss, *Chem. Phys. Lett.* **157**, 200 (1989).

[29] M.E. Casida, C. Jamorski, K.C. Casida, D.R. Salahub, *J. Chem. Phys.* **108**, 4439 (1998).

[30] S. Resan, R. Hameed, A. Al-Hilo, M. Al-Anber, *Revista. Cubana de Física* **37, 95 (2020)**.

[31] A.K. Biswas, S. Barik, A. Sen, A. Das, B. Ganguly, *J. Phys. Chem. C* **118**, 20763 (2014).

[32] A.K. Biswas, A. Das, B. Ganguly, *Int. J. Quantum Chem.* **117**, e25415 (2017).

[33] M. Lazrak, H. Toufik, S.M. Bouzzine, F. Lamchouri, *Res. Chem. Intermed.* **46**, 3961 (2020).

[34] R. Hoffmann, *Acc. Chem. Res.* **4**, 1 (1971).

[35] A.K. Biswas, A. Das, B. Ganguly, *New J. Chem.* **40**, 9304 (2016).

[36] A. Mahmood, S.U.D. Khan, U.A. Rana, *J. Comput. Electron.* **13**, 1033 (2014).

[37] Y. Li, Y. Li, P. Song, F. Ma, J. Liang, M. Sun, *RSC Adv.* **7**, 20520 (2017).

[38] Z.M.E. Fahim, S.M. Bouzzine, M. Hamidi, *Res. Chem. Intermed.*, **44**, 2009 (2017).

[39] C. Sun, Y. Li, P. Song, F. Ma, *Materials (Basel)* **9**, 813 (2016).

[40] R. Nithya, K. Senthilkumar, *Phys. Chem. Chem. Phys.* **16**, 21496 (2014).

[41] J. Preat, C. Michaux, D. Jacquemin, E.A. Perpčte, *J. Phys. Chem. C* **113**, 16821 (2009).

[42] F.-Q. Bai, M. Xie, H.-X. Zhang, Y.-Q. Zheng, *J. Mater. Chem. B* **3**, 6871 (2015).

[43] M. Xie, L. Hao, R. Jia, J. Wang, F.Q. Bai, *New J. Chem.* **43**, 651 (2019).

[44] Z. Yang, C. Liu, C. Shao, C. Lin, Y. Liu, *J. Phys. Chem. C* **119**, 21852 (2015).

[45] M. Karuppusamy, V. Surya, K. Choutipalli, D. Vijay, V. Subramanian, *J. Chem. Sci.* **132**, 2039 (2020).

[46] B. Kippelen, J.L. Brédas, *Energy Environ. Sci.* **2**, 251 (2009).